Methane-derived authigenic carbonates – A case for a globally relevant marine carbonate factory

Sajjad A Akam[1], Elizabeth D Swanner[1], Hongming Yao[2], Wei-Li Hong[3], Jörn Peckmann[4]

1 Department of Geological and Atmospheric Sciences, Iowa State University, Ames, IA, USA 50014

2 Shenzhen Engineering Laboratory for Big Data Analysis and Application of Ocean Environment, Shenzhen Institute of Advanced Technology Chinese Academy of Sciences, 518055, China

3 Department of Geological Sciences, Stockholm University, 106 91, Stockholm, Sweden

4 Institute for Geology, Center for Earth System Research and Sustainability, Universität Hamburg, 20146 Hamburg, Germany

sajjad@iastate.edu

Abstract:

Precipitation of methane-derived authigenic carbonates (MDAC) is an integral part of marine methane production and consumption, but MDAC's relative significance to the global marine carbon cycle is not well understood. Here we provide a synthesis and perspective to highlight MDAC from a global marine carbon biogeochemistry viewpoint. MDAC formation is a result and archive of carbon-sulfur (C-S) coupling in the shallow sulfatic zone and carbon-silicon (C-Si) coupling in deeper methanic sediments. MDAC constitute a carbon sequestration of 3.93 Tmol C yr^{-1} (range 2.34–5.8 Tmol C yr^{-1}) in the modern ocean and are the third-largest carbon burial mechanism in marine sediments. This burial compares to 29% (11–57%) organic carbon and 10% (6–23%) skeletal carbonate carbon burial along continental margins. MDAC formation is also an important sink for benthic alkalinity and, thereby, a potential contributor to bottom water acidification. Our understanding of the impact of MDAC on global biogeochemical cycles has evolved over the past five decades from what was traditionally considered a passive carbon sequestration mechanism in a seep-oasis setting to what is now considered a dynamic carbonate factory expanding from deep sediments to bottom waters—a factory that has been operational since the Precambrian. We present a strong case for the need to improve regional scale quantification of MDAC accumulation rates and associated carbonate biogeochemical parameters, leading to their incorporation in present and paleo-carbon budgets in the next phase of MDAC exploration.

Introduction

Carbon is primarily buried in marine sediments as carbonate and organic carbon, which removes carbon from the water column and the biological carbon cycle to the vast but slower geological carbon cycle within sediments (Falkowski et al., 2000). Marine sediments also host the largest reservoir of methane (CH_4), a potent greenhouse gas largely produced by microbial and thermocatalytic degradation of buried organic carbon, with an estimated carbon pool size that is similar to or significantly higher than the conventional oil and gas reservoir (Ciais et al., 2013; Bohrmann and Torres, 2014). Continental margins are characterized by the transfer of methane (and other hydrocarbons) in dissolved and gaseous forms via diffusion and advection from subsurface reservoirs to the seafloor, which reconnects the methane-carbon buried in deeper sediments back to faster carbon cycling in shallow sediments, water column, and atmosphere (Talukder, 2012). While the direct role of sedimentary methane fluxes on paleoclimate perturbations remains largely unresolved (Dickens, 2011; Ruppel and Kessler, 2017), methane production, transport, oxidation, and assimilation of methane-derived carbon by biota generate a highly interactive geobiological setting that can sustain some of the richest deep-sea ecosystems and impact the sedimentary as well as water column biogeochemistry at regional to global scales (Judd and Hovland, 2007; Levin et al., 2016; Akam et al., 2020) (Fig. 1).

Formation of methane-derived authigenic carbonates (MDAC) is a major part of the methane-driven carbon cycling in marine sediments (Peckmann and Thiel, 2004; Naehr et al., 2007) (Fig. 1). We define MDAC as authigenic carbonate minerals precipitated in situ within marine sediments, seafloor, or bottom water with dissolved inorganic carbon (DIC) derived primarily from (i) anaerobic oxidation of methane (Eqns. 1 and 4) and (ii) methane production, the latter linked to marine silicate weathering in methanic sediments (Eqns. 2-4). In the equations below, we do not differentiate the different speciation of aqueous carbonate ions but concern only the mass balance of bulk DIC. These equations, thus, cannot be used to assess the associated alkalinity changes. Such a decision is a result of the poorly constrained DIC-to-alkalinity ratios when equations 1-4 are collectively considered (refer to section 5).

$$CH_4 + SO_4^{2-} \rightarrow HCO_3^- + HS^- + H_2O. \qquad (1)$$

$$2CH_2O \xrightarrow{+2H_2O} 2CO_2 + 4H_2 \xrightarrow{-2H_2O} CO_2 + CH_4 \qquad (2)$$

$$\text{Cation} - \text{rich silicate} + CO_2 + H^+ \rightarrow \text{Cation} - \text{depleted silicates} + HCO_3^- + \text{Cations} \qquad (3)$$

$$2HCO_3^- + Ca^{2+} + \text{dissolved cations} \rightarrow Ca(Fe, Mg, Mn, Ba)\,CO_3 + H_2O + CO_2 \qquad (4)$$

MDAC have been recognized since the 1960s and remain an active research frontier (Hathaway and Degens, 1969; Claypool and Kaplan, 1974; Suess, 2014; Hong et al., 2022). Research on

seep and other methane-derived carbonates, their isotopic and trace element signatures, molecular and bodyfossil records, and petrographic signatures has helped in characterizing seepage and its geologic record (Peckmann and Thiel, 2004; Campbell, 2006; Roberts and Feng, 2013; Suess, 2014; Smrzka et al., 2021). MDAC can be commonly distinguished from skeletal carbonate through their negative carbon stable isotopic signatures ($\delta^{13}C_{carbonate}$) inherited from methane—where methane production and oxidation are characterized by ^{13}C enrichment and depletion, respectively (Naehr et al., 2007; Meister and Reyes, 2019). Here we provide a perspective and synthesis that evaluates the role of MDAC dynamics in global marine carbon burial quantitatively. Formation of MDAC is not only an important carbon sequestration mechanism and a geologic recorder of methane seepage but also a dynamic carbonate factory that has been operational through much of geological history with a spatial sphere of influence expanding from deeply buried sediments to bottom water columns.

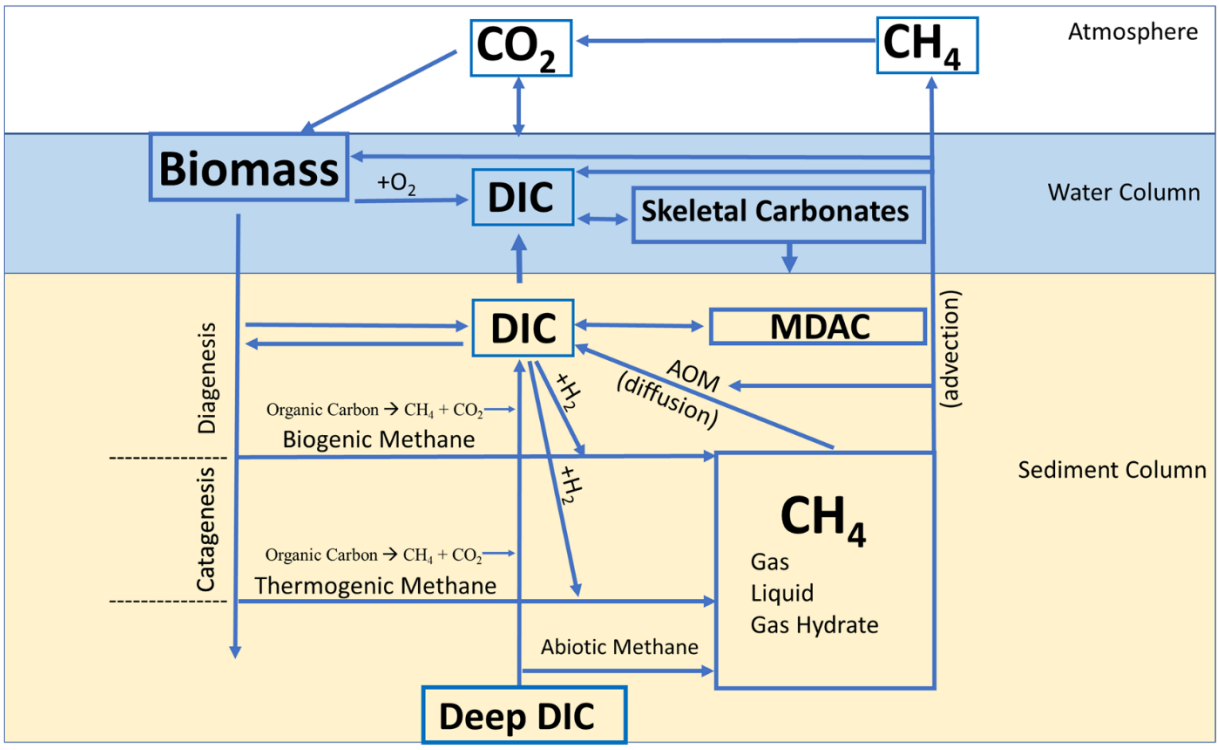

Figure 1: A simplified representation of methane as an intermediate in marine carbon cycling and the role of methane-derived carbonates in these processes.

1. A case for C-S and C-Si coupling in marine sediments archived in the rock record

MDAC in shallow sulfatic sediments beneath the modern ocean are primarily a result of microbial sulfate-dependent anaerobic oxidation of methane (SD-AOM; Eqn. 1) occurring in the sulfate-methane transition zone (SMTZ, Fig. 2), the diagenetic front where the upward migration

of methane encounters the downward diffusive sulfate flux (Reeburgh, 1976; Borowski et al., 1996). SD-AOM is the dominant form of AOM since sulfate (28 mM) is the most abundant electron acceptor for anaerobic oxidation of methane in the modern ocean (Jørgensen and Kasten, 2006; Egger et al., 2018). SD-AOM results in carbonate precipitation with characteristic ^{13}C depletion (Naehr et al., 2007; Meister and Reyes, 2019). Recent compilations on global methane diffusive transport suggest that methane-charged sediments are predominantly located in shelf and slope setting with water depth <2000 m, constituting >90% of methane and sulfate fluxes, with a shallow average SMTZ depth ≤ 13 meters below seafloor (Egger et al., 2018). Hence SD-AOM-induced MDAC represent an archive for carbon-sulfur (C-S) coupling in shallow marine sediments impacted by subsurface methane transport (Eqns 1, 4). Authigenic carbonates in sulfatic sediments can also be formed from C-S cycling via microbial organoclastic sulfate reduction (OSR; $2CH_2O + SO_4^{2-} \rightarrow H_2S + 2HCO_3^-$) and via sulfate reduction coupled to non-methane hydrocarbons including crude oil components (Smrzka et al., 2019; Akam et al., 2021). A global account of authigenic carbonate formation via OSR in non-methane-laden sediments and oxidation of non-methane hydrocarbons compounds is poorly constrained and not considered here. We focus on diffusion-controlled methane-laden sediments where comparative analyses of authigenic carbonate formation in global marine sediments via SD-AOM vs. OSR suggest methane consumption is a key driver of carbonate alkalinity in the sulfatic zone and hence MDAC formed through SD-AOM is the dominant form of authigenic carbonate formation via C-S coupling (Meister et al., 2013; Bradbury and Turchyn, 2019; Akam et al., 2020; Zhang, 2020; Turchyn et al., 2021; Loyd and Smirnoff, 2022).

In methanic sediments (below the SMTZ), MDAC are also an archive of C-Si coupling in deeper sediments (Fig. 2): Eqn. 2 considers both acetoclastic and autotrophic methanogenesis where net organic matter fermentation and carbon dioxide (CO_2) reduction are balanced with equivalent amounts of CO_2 and CH_4 produced per mole of organic matter degraded at steady-state (Eqns. 5–9) (Solomon et al., 2014; Meister et al., 2019).

$$2CH_2O + 2H_2O \rightarrow 2CO_2 + 4H_2 \text{ (Carbohydrate Fermentation)} \quad (5)$$

$$2CH_2O \rightarrow CH_3COO^- + H^+ \text{ (Carbohydrate Fermentation)} \quad (6)$$

$$CO_2 + 4H_2 \rightarrow CH_4 + 2H_2O \text{ (CO_2 Reduction)} \quad (7)$$

$$CH_3COO^- + H^+ \rightarrow CH_4 + CO_2 \text{ (Acetate Fermentation)} \quad (8)$$

$$2CH_2O \rightarrow CH_4 + CO_2 \text{ (Net Reaction)} \quad (9)$$

The CO_2 produced with CH_4 in the methanogenic zone lowers the pH and favors dissolution/weathering of silicate minerals by carbonic acid (Aloisi et al., 2004). The combined effect of fermentation and marine silicate weathering (MSiW; Eqn. 3) in methanic sediments results in a favorable condition for carbonate precipitation along with an upward DIC and cation

flux toward the sulfatic zone (Solomon et al., 2014; Torres et al., 2020) (Eqns. 2–4 Fig. 2). Such DIC contribution from methanogenesis is evident by ^{13}C enrichment of authigenic carbonates, a characteristic by-product of methanogenesis where methane preferentially incorporates ^{12}C, leaving behind ^{13}C-enriched DIC (Boehme et al., 1996; Meister and Reyes, 2019). Taken together, MDAC in the sediment column represents C-S coupling in the shallow sulfatic zone and C-Si coupling in deeper methanic sediments (Fig. 2). Further, these two processes, MDAC formation in the sulfatic and methanogenic zones, are highly interconnected since the C-Si coupling through MSiW has a strong control on the amount of DIC and alkalinity entering the shallow sediments for MDAC formation via C-S coupling. The extent of DIC mixing from the sulfatic and methanogenic zones would also have a strong control on the $\delta^{13}C$ values of shallow MDAC and their identification using isotopic signals (E.g., Hong et al., 2014).

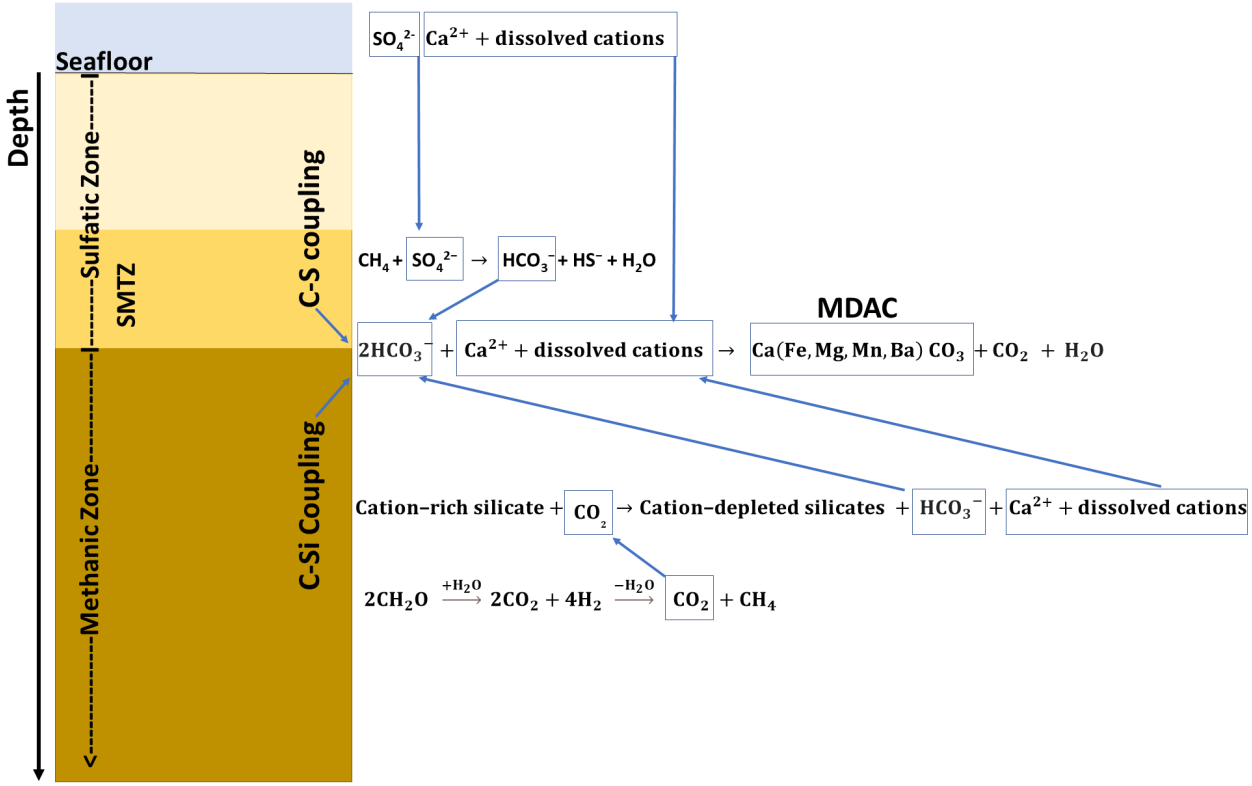

Figure 2: A simplified representation of MDAC formation by carbon-sulfur (C-S) cycling in methane-charged shallow sulfatic zone via anaerobic oxidation of methane (AOM) and via carbon-silica (C-Si) coupling in deeper methanic sediments via methanogenesis coupled with marine silicate weathering (MSiW). SMTZ represents sulfate-methane transition zone. Note that MDAC form throughout sediment affected by anaerobic methanotrophy and methanogenesis; organoclastic sulfate reduction also induces carbonate formation in shallow sediments but is not shown in the figure in order to focus on the methane-driven processes.

2. Global MDAC reservoir in the modern ocean

Globally, carbonate authigenesis has been proposed as the third major marine carbon sink after organic carbon and skeletal carbonate burial (Schrag et al., 2013). MDAC formation is the dominant process of carbonate precipitation in marine sediments (Loyd and Smirnoff, 2022). However, there is only a handful of attempts to quantify MDAC carbon burial in the modern oceans (e.g., Wallmann et al., 2008; Sun and Turchyn, 2014; Bradbury and Turchyn, 2019; Akam et al., 2020). The most recent estimate of the global MDAC reservoir size in the sulfatic zone (Akam et al., 2020) derived from the assumption of the quantitative oxidation of the estimated global diffusive CH_4 flux of 2.8–3.8 Tmol CH_4 yr^{-1} (Egger et al., 2018), suggested a MDAC induced carbon sequestration of 1.7 Tmol DIC yr^{-1} with a range from 0.6–3.6 Tmol DIC yr^{-1} (following Eqns. 1 and 4).

In a more recent compilation of porewater data of 242 sites from the South China Sea combined with existing global extrapolation techniques, an updated quantification of global diffusive CH_4 flux ranges from 5.0 to 6.5 Tmol CH_4 yr^{-1} (Hu et al., 2022; Hu et al., 2023). This higher estimate is attributed to previously unaccounted 2.18–2.65 Tmol CH_4 yr^{-1} deep-sourced (non-steady state) diffusive methane flux in continental slope and rise settings. This estimate of deep-sourced CH_4 based on sulfate reduction rates also agrees with a previous independent estimate based on a mismatch between the amounts of CH_4 generated and consumed in continental slope sediments (Boetius and Wenzhöfer, 2013). Plugging the updated CH_4 and SO_4^{2-} flux values into the carbon flux model of Akam et al. (2020) yields a DIC sequestration of 2.28 (range: 1.34–5.37) Tmol C yr^{-1} via MDAC in sulfatic sediments (Supp. section 1). How much of this DIC will eventually be sequestrated as MDAC is not fully resolved because of existing uncertainties regarding the effect of different biogeochemical processes in methane-charged sediment settings towards carbonate alkalinity and speciation of aqueous carbonate ions. While AOM plays a crucial role in increasing the TA/DIC ratio necessary for carbonate precipitation (Meister, 2013), carbonate precipitation can be limited by multiple factors, including dissolution, changes in methane flux velocity, sedimentation rates, bioturbation, etc. (Luff et al., 2004; Bayon et al., 2007). Notably, according to Eq. 4, Two moles of bicarbonate ion form one mole of carbonate mineral and one mole of CO_2. The CO_2 releases, or in the form of carbonic acid, will acidify porewater and makes carbonate minerals more difficult to form. These factors are considered in the recent methane-carbon flux budget by Akam et al. (2020), which adopted a conservative estimate of 20% (10–35%) of total DIC through the SMTZ is being sequestered as MDAC (Supp. Table 1), while reported regional values indicate a DIC sequestration up to 66% (Smith and Coffin, 2014; Chuang et al., 2019). Further, even with the conservative estimate, if we assume the 2:1 stoichiometry of DIC to $CaCO_3$ in equation 4, the MDAC pool in sulfatic sediments shaped by AOM accounts to for 1.14 (0.67–2.69) Tmol $CaCO_3$ yr^{-1}.

While the above estimates target MDAC formation via C-S coupling in shallow sulfatic sediments at and above the SMTZ, quantification of the total MDAC accumulation is only complete if one considers MDAC formation in the methanogenic zone via C-Si coupling (Eqn.

2-4, Fig. 2). Based on the stoichiometry from Eqn. 2 and a global methanogenesis rate of 2.8–3.8 Tmol CH_4 yr^{-1} (Egger et al., 2018), an equal amount of CO_2 (i.e. 2.8–3.8 Tmol CO_2 yr^1 is generated in the methanogenic zone. Following the extensive literature survey based assumption pointing to about 50% (1.4–1.9 Tmol C yr^{-1}) of this CO_2 being converted to carbonate alkalinity that induces precipitation of carbonate in the deep methanic sediments and the remainder diffuses up to the shallow sediments (Akam et al., 2020), MDAC formation in deeper methanic sediments (below the SMTZ) accounts for an additional 1.4–1.9 Tmol C yr^{-1} DIC sequestration and a carbonate pool of 0.70–0.95 Tmol $CaCO_3$ yr^{-1} (Eqn. 4). Since there are no global constraints available for deep-DIC flux associated with deep-sourced methane in non-steady state setting, we have only considered the steady-state methanogenic DIC (2.8–3.8 Tmol C yr^{-1}) in the MDAC estimates in methanic sediments, hence it is a conservative estimate. The deeper-MDAC formed in methanic sediments may appear to be unconnected to the shallow system; however, since the amount of MDAC formation at depth controls the deeper flux of DIC, alkalinity, and cations to the shallow sediments and the seafloor (Berg et al., 2019; Akam et al., 2020; Torres et al., 2020) (Fig.2), it is coupled with the oceanic DIC cycle. Overall, the total DIC sequestration due to MDAC formation in marine sediments across shallow sulfatic and deeper methanic sediments is 3.93 (3.67–4.18; extended range: 2.34–5.80) Tmol C yr^{-1} (2.28 Tmol C yr^{-1} sequestered at sulfatic sediments explained in the previous paragraph and 1.4–1.9 Tmol C yr^{-1} sequestered at methanic sediments below SMTZ; Supp info) – this value quantitatively affirms MDAC as the third major carbon sink in modern marine sediments.

The 2:1 stoichiometry of DIC to $CaCO_3$ in equation 4 would yield an average carbonate accumulation rate of 1.97 $CaCO_3$ yr^{-1} – a twofold increase in authigenic carbonate burial than the currently most cited estimate on authigenic carbonate formation (1 Tmol C yr^{-1}) (Sun and Turchyn, 2014). We attribute this disparity to two key factors; (i) consideration of deep-DIC flux of alkalinity and cations to the sulfatic zone need to consider Mg^{2+} and other cation fluxes along with Ca^{2+} flux contributing to carbonate [Ca (Fe, Mg, Mn, Ba) CO_3] precipitation, and (ii) the greater availability of porewater data for the upper 1.5 m of sediments considered in this study (primarily from Egger et al., 2018), often ignored in previous ODP/DSDP/ IODP based estimates. Interestingly, our estimates are close to the average value of the range of MDAC accumulation estimates of Torres et al. (2020; 1–4 Tmol C yr^{-1}), which also considered MDAC formation in the methanogenic zone. Figure 3 shows the MDAC distribution pattern in continental margin sediments derived from an interpolation at 0.1 x 0.1° resolution based on published data of diffusive fluxes of methane and sulfate from 542 global sites. We expect future development of such global patterns will provide a baseline for more precise ground truthing and refinement of regional MDAC budgets. Our MDAC quantification here is still a conservative estimate since the flux of non-steady state diffusive and advective CH_4 transport from deeper hydrate-bearing sediments as well as in the abyssal ocean is largely unconstrained (Boetius and Wenzhöfer, 2013; Marlow et al., 2022). Furthermore, a recent work by Xu et al. (Xu et al., 2022) suggested that the DIC production from depth-integrated AOM could be as high as 8.9 Tmol C yr^{-1} —which could increase the MDAC accumulation rates to higher values than what is considered here.

Our estimate of MDAC accumulation rates equates to 29% (11–57%), 5% (1–15%), and 27% (9–55%) of organic carbon burial in continental margins, abyss, and global marine sediments, respectively. MDAC accumulation rates are comparable to 10% (6–23%), 0.3% (0.2–0.4%), and 7% (4–13%) of the burial of skeletal carbonate along continental margins, abyssal plains, and global marine sediments, respectively (Table 1 and Supp info). Depending on the global sulfate reduction estimate of 75 Tmol SO_4^{2-} yr^{-1} (Jørgensen and Kasten, 2006) or 11.3 Tmol SO_4^{2-} yr^{-1} (Bowles et al., 2014), MDAC accumulation in sulfatic sediments will account for the sequestration of 3–24% of the total DIC produced in shallow marine sediments due to sulfate reduction. In addition, MDAC accumulation corresponds to 63% (38–94%) of 3.1 Tmol $CaCO_3$ yr^{-1} detrital carbonate minerals discharged to oceans (Müller et al., 2022), five times higher (312%–773%) than the 0.5–1 Tmol C yr^{-1} alkalinity sink via reverse weathering (Isson and Planavsky, 2018), and 131% (78–193%) of the 1.5–2.4 Tmol $CaCO_3$ yr^{-1} accumulation in the oceanic crust (Alt and Teagle, 1999; Supp. Table 4).

While not considered in the reservoir calculations above, it is also noteworthy that MDAC forms as cap rocks in deep hydrocarbon systems (Caesar et al., 2019). The suggested volume for onshore salt domes only in the Gulf of Mexico basin is 6.75 Gt C (sequestering 9 Gt CH_4; Caesar et al., 2019). Similar systems exist in other cap rocks (e.g., Labrado et al., 2019, and references therein). MDAC formation would have been much greater during anoxic events than at present (Higgins et al., 2009; Yao et al., 2022), but is still significant for the modern ocean. Despite their volumetric and biogeochemical significance from a bottom-up carbon flow perspective, MDAC is not well-recognized as a major carbonate factory (Andersson, 2014; Michel et al., 2019).

Organic carbon analysis suggests that shallow MDAC are also an effective sequesterer of organic matter sourced from seep biota (Peckmann and Thiel, 2004) and autoendolithic activities (Marlow et al., 2021). A recent study by Feng et al. (2021) evaluated the total organic carbon (TOC) content of MDAC from the Gulf of Mexico and the South China Sea and observed consistently high TOC contents (average 1.22 wt%). Interestingly, only 20% of this TOC showed modern ^{14}C age, and the remaining 80% TOC with 0% modern carbon also showed ^{13}C depletion, pointing to sizable organic carbon incorporation onto MDAC from methane-cycling biota. Considering an average 1.14 (0.67–2.69) Tmol $CaCO_3$ yr^{-1} shallow MDAC accumulation, such organic carbon preservation trend implies an approximate 1×10^{-2} (6×10^{-3} – 3×10^{-2}) Tmol organic carbon is being sequestered in shallow MDAC annually.

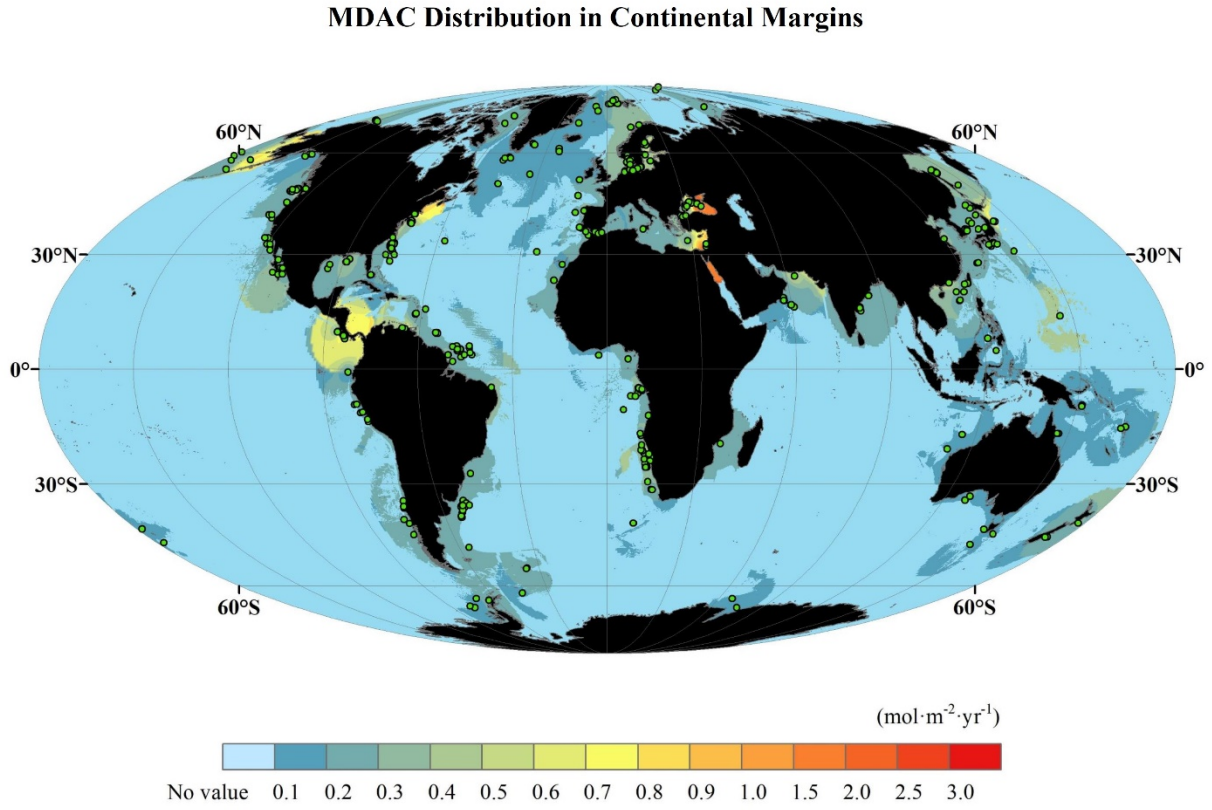

Figure 3: MDAC accumulation rates in mol $CaCO_3$ m^{-2} yr^{-1} on continental margins derived from an interpolation at 0.1 x 0.1° resolution based on published data of diffusive methane and sulfate flux (Egger et al., 2018) from 542 global sites with water depth <4000m.

Table 1: Major carbon burial mechanisms in marine sediments compared with MDAC accumulation. Organic carbon burial and DIC sequestration via MDAC values are in Tmol C yr^{-1}. Carbonate burial values are in Tmol $CaCO_3$ yr^{-1}. The carbonate and organic carbon burial volumes are summarized from a range of published global estimates. Refer to Supp. Information for details.

Region (water depth in m)	OC Burial	Carbonate Burial	Total Burial	Shallow MDAC	Deep MDAC	Total MDAC	Total MDAC compared to		
							%OC Burial	%Carb Burial[#]	%Total Burial
Margins (<3500)	13.20	18.50	31.70	2.25	1.61	3.86	29%	10%	12%
Abysall (>3500)	1.30	11.10	12.40	0.03	0.04	0.07	5%	0.3%	0.6%
Total	14.50	29.60	44.10	2.28	1.65	3.93	27%	7%	9%

[#]2 moles of DIC consumed to form 1 mole of $CaCO_3$

3. Methane-derived carbon sequestration and a connection to ocean acidification

The influence of benthic DIC fluxes on ocean carbon chemistry and ocean acidification has gained significant scientific attention recently (e.g., Thomas et al., 2008; Hu and Cai, 2011; Krumins et al., 2013; Brenner et al., 2016; Middelburg et al., 2020; Santos et al., 2021). While numerous factors (e.g., submarine groundwater discharge, organic matter degradation, carbonate, iron sulfide burial, etc.) have been suggested as controlling factor for the benthic alkalinity flux, MDAC are probably another strong control. Notably, Hu and Cai (2011) mentioned in their synthesis of global benthic alkalinity flux that the lack of global MDAC precipitation rates limits their inclusion in existing benthic alkalinity models and any assessment of the role of MDAC in ocean acidification. A similar case, where the potential of seep-induced carbonate chemistry could be a major unquantified driver of ocean acidification, was highlighted in a recent review of ocean acidification dynamics in the Gulf of Mexico (Osborne et al., 2022). The development of global MDAC estimates is a positive step in that direction. While often highlighted as a carbon sequestration mechanism that prevents a portion of the methane flux from directly interacting with the water column and the atmosphere, MDAC formation can also influence bottom water carbonate chemistry and thereby ocean acidification. This is largely because subsurface methane transport is associated with a significant amount of benthic DIC flux to the water column (Zhang et al., 2019; Akam et al., 2020; Fig. 4). The average global DIC outflux from marine sediments toward the water column due to diffusive methane transport is 6.5 Tmol C yr^{-1} (range: 3.2–9.2 Tmol C yr^{-1}), corresponding to 20% of the global riverine DIC flux to the oceans (Akam et al., 2020). While AOM is a source of this benthic DIC flux, MDAC formation acts as a DIC sink. Further, authigenic carbonate formation consumes 2 moles of alkalinity for every mole of $CaCO_3$ formation and hence lowers the total alkalinity (TA) to DIC ratio (TA/DIC) of benthic DIC outflux to the water column. The deeper MDAC forming in the methanogenic zone results in CO_2 production and, thus, acidification of pore fluids. Such an effect may pose a positive feedback for MSiW, which is nonetheless poorly constrained by a limited number of studies on MSiW (Aloisi et al., 2004; Wallmann et al., 2008; Solomon et al., 2014; Torres et al., 2020; Meister et al., 2022). The formation of deep MDAC is also attenuating the alkalinity flux toward shallow sulfatic sediments – the higher the deep MDAC formation, the lower the alkalinity contribution to shallow sediments from below. Further, 97% (3.65 Tmol yr^{-1}) of the total 3.8 Tmol yr^{-1} MDAC is formed in shelf and slope settings (<2000 m water depth) with an average SMTZ depth of <13 mbsf (Egger et al., 2018). Recent studies have suggested that anthropogenically influenced higher organic carbon loading to coastal systems can enhance methanogenesis and shoaling of the SMTZ (Jilbert et al., 2021). A large amount of MDAC formation at sites with shallow SMTZ depth implies a potentially stronger impact on bottom water chemistry and contemporaneous carbon cycling.

MDAC dissolution, on the other hand, contributes alkalinity to the water column. Initial estimates of shallow MDAC dissolution via sulfide oxidation is 0.06 ± 1 Tmol yr^{-1} (Leprich et al., 2021). However, the key processes driving MDAC dissolution—aerobic methane oxidation ($CH_4 + 2O_2 \rightarrow CO_2 + 2H_2O$) and aerobic sulfide oxidation ($H_2S + 2O_2 \rightarrow SO_4^{2-} + 2H^+$)—contribute to ocean

acidity (e.g., Cordova-Gonzalez et al., 2023). In addition, shallow MDACs precipitate not only interstitially within the sediment but also in the pore space of rocks by methanotrophic autoendoliths (Marlow et al., 2021). Considering the widespread accumulation of MDAC in shallow sediments impacted by subsurface methane fluxes across continental margins (Naehr et al., 2007; Suess, 2014), it is reasonable to assume a reduction in methane-driven benthic alkalinity flux due to MDAC precipitation that is not well characterized at present. Hence, there is a need to quantify the contribution of biogeochemical processes occurring in methane-bearing sediments to the TA/DIC ratio and constrain the role of these processes to bottom water carbonate chemistry.

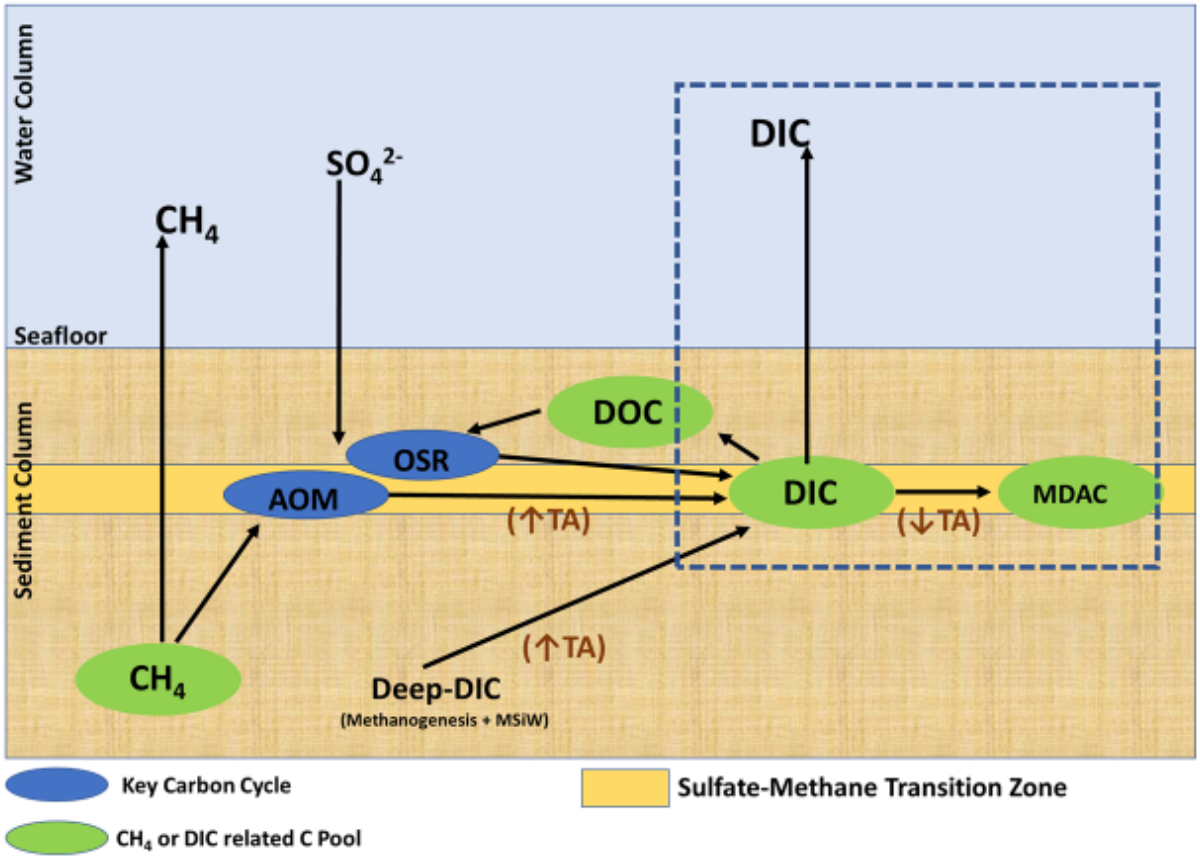

Figure 4: Benthic flux of dissolved inorganic carbon (DIC) to the water column from methane-charged sediments. The dashed box highlights the role of MDAC in controlling the TA:DIC ratio of this DIC outflux. MDAC formation will consume alkalinity and reduce TA:DIC of this benthic DIC flux. MDAC dissolution will increase TA:DIC. Widespread MDAC accumulation in ocean margins indicate the lowering of TA/DIC dominates in modern oceans and future studies need to constrain these TA:DIC dynamics at subsurface methane transport settings. Figure adapted from Akam et al..

4. Paleo-perspective

The steadily increasing number of paleo-seep studies points to MDAC as the dominant mode of authigenic carbonate formation in the geological past (Campbell, 2006; Peckmann et al., 2011; Haig et al., 2022). The methane reservoir is considered to have been a major marine carbon reservoir since the Archean (Kharecha et al., 2005; Haqq-Misra et al., 2008), and methane-related carbon cycling and MDAC formation is also likely to have been a relevant component of marine carbon chemistry for most of Earth's history. There is growing evidence that MDAC formation was affected by glacial-interglacial transitions (Chen et al., 2019; Oppo et al., 2020). A recent global compilation across 150 million years by Oppo et al. (2020) provides support for sea-level forcing and rates of organic carbon burial as the main factors controlling overall methane transport and MDAC formation. There is also growing evidence for methane flux control and MDAC formation owing to hydrological and tidal plumbing, bottom water warming, glacio-isostatic loading, as well as seismic, tectonic, and stratigraphic variability (Roberts and Carney, 1997; Maslin et al., 1998; Suess, 2014; Portnov et al., 2016; Wallmann et al., 2018; Chen et al., 2019; Prouty et al., 2020). While the individual processes at play causing these flux variations are beyond the scope of this discussion, flux variations will directly impact the methane-carbon cycling and the size of the MDAC pool. The cause-effect relationship of such processes over different spatiotemporal scales and their associated impact on bottom-up carbon dynamics via methane-DIC and MDAC is largely overlooked and presents as an emerging paleoceanographic challenge.

The record of ^{13}C-depleted MDAC is continuous in the geological record from 360 Ma onward (Campbell, 2006), a time frame that also matches the secular variation of global marine sulfate concentration becoming high enough to sustain SD-AOM (Bristow and Grotzinger, 2013). The traditional MDAC search strategy is based on examples from modern, Cenozoic, and Mesozoic seep deposits characterized by high seawater sulfate and DIC concentrations permitting rapid MDAC precipitation driven by SD-AOM with ^{13}C depletion and distinctive fabrics (Peckmann and Thiel, 2004; Bristow and Grotzinger, 2013). The specific role of MDAC during low oxygen and/or low sulfate states of Earth is less understood. Currently, there are only limited examples of such ^{13}C-depleted seep carbonate signatures in deep time, notably from south China – the Neoproterozoic examples of basal Ediacaran cap dolostone (Jiang et al., 2003; Peng et al., 2022), upper Ediacaran carbonates from the Doushantuo formation (Cui et al., 2017), and dolomites from a lower Cambrian organic-rich succession (Zhou et al., 2022). Some Neoproterozoic and Paleozoic seep carbonates lack diagnostic $\delta^{13}C_{carbonate}$ depletion, but their seep setting has been verified via evidence from geological context, fabrics, and fossil assemblages (e.g., Peckmann et al., 2007; Kennedy et al., 2008; Jakubowicz et al., 2017). Evidence for AOM-related MDAC from Precambrian through early Paleozoic could have ambiguous $\delta^{13}C_{carbonate}$ values due to lower sulfate and DIC concentrations and carbon cycle perturbations that led to positive carbon isotope anomalies (Bristow and Grotzinger, 2013). Further, the mixing of different DIC pools commonly masks the $\delta^{13}C$ signals of methane-derived DIC (Peckmann and Thiel, 2004). Hence MDAC formation, their geochemical fingerprinting, and the impact on $\delta^{13}C_{carbonates}$ and carbon cycling

throughout geological history, especially the Precambrian and early Paleozoic, remains largely unexplored (Saitoh et al., 2015).

Recent developments provide insight into what could have been at play with regards to MDAC in Precambrian oceans. Authigenic carbonates have been postulated as a globally relevant carbon pool during ocean anoxia of the Archean and Proterozoic (Higgins et al., 2009; Schrag et al., 2013). MDAC could have precipitated in the anoxic water column and sediments through multiple pathways in redox-stratified early oceans. A low sulfate ocean favoring enhanced methanogenesis combined with methane seepage reaching the atmosphere to a higher degree and/or high ocean alkalinity events, resulting in ^{13}C-enriched MDAC accumulation at regional or global scale, has been suggested as a cause for Paleoproterozoic positive carbon isotope excursions (Hayes and Waldbauer, 2006; Birgel et al., 2015; Cadeau et al., 2020). Methanogenic DIC is invoked as a possible sourcing for the Proterozoic molar tooth structures, crenulated carbonate fabrics characterized by rapid calcitic microspar filling of cracks and voids within unconsolidated sediments (Frank and Lyons, 1998; Shen et al., 2016; Kriscautzky et al., 2022; Tang et al., 2023). Additionally, the enhanced burial of ^{13}C-enriched MDAC driving a depletion of global oceanic $^{13}C_{DIC}$ and/or regionally enhanced formation of ^{13}C-depleted MDAC affecting the $^{13}C_{DIC}$ of restricted basins have been proposed as potential causes for Neoproterozoic negative carbon isotope excursion (Schrag et al., 2013; Laakso and Schrag, 2020; Cui et al., 2022).

Methanotrophy-derived MDAC could have formed through multiple pathways on an early Earth. Iron-driven AOM can produce MDAC in modern (Himmler et al., 2010; Sun et al., 2015; Peng et al., 2017) and potentially in the ancient oceans (Bekker et al., 2010). A case for manganese-driven AOM producing MDAC has been made for the Jurassic Franciscan Complex in California (Hein and Koski, 1987) and for the Triassic Junggar Basin in northwestern China (Cai et al., 2021). The Black Sea and Makran margins serve as examples for MDAC formation by AOM in anoxic bottom waters, occurring beneath chemoclines in stratified water bodies (Michaelis et al., 2002; Himmler et al., 2016). Recent evidence from ferruginous (anoxic and iron-rich) lakes, representative of the Archean ocean as well as the deeper ocean in the Proterozoic (Swanner et al., 2020), finds that ^{13}C-depleted manganese carbonates are being formed at the chemocline with aerobic methanotrophy sourcing the ^{13}C-depleted DIC (Wittkop et al., 2020). While aerobic methanotrophy does not produce MDAC in the present ocean—instead, it causes dissolution (Matsumoto, 1990; Cordova-Gonzalez et al., 2023) —the ancient Earth would have had MDAC formation through aerobic methanotrophy at chemoclines (Wittkop et al., 2020). Some of the Precambrian carbonates [Ca (Fe, Mg, Mn) CO_3] could thus be in fact MDAC (Schrag et al., 2013; Birgel et al., 2015; Lepot et al., 2019). For Phanerozoic, early Cretaceous, anoxia events, the role of methane-driven carbon cycling was deduced based on evidence from ^{13}C depletion in carbonates along with increased Mn contents of carbonates (Renard et al., 2005). These findings call for revisiting Precambrian and Phanerozoic sedimentary manganese- and iron-rich carbonates, which may have formed from methane-derived DIC (Renard et al., 2005; Bekker et al., 2010; Wittkop et al., 2020; Cai et al., 2021). Paleo-records indicating enhanced methanogenesis, methane fluxes, and MDAC formation during oceanic anoxic events also

suggest that the ongoing decline of oxygen in the global ocean waters (Breitburg et al., 2018), as well as the projected expansion of oxygen minimum zones (Cavicchioli et al., 2019), will probably increase MDAC formation in the future (Oppo et al., 2020; Yao et al., 2022). Such evolving concept suggests that MDAC had been a significant part of global carbon biogeochemistry throughout Earth's history and will likely be a significant component of future oceans as well.

5. Future work

Future work needs to constrain the contribution of methane-derived DIC being incorporated into MDAC in diverse methane-laden environments. Existing reservoir estimates consider an average 20–33% of shallow DIC and 33–50% of methanogenic DIC being sequestered as MDAC, based on an available global compilation (Akam et al., 2020; Torres et al., 2020). Future refinement of DIC fluxes in diverse methane-flux settings will improve these estimates. Fluid flow velocity is also an important factor – it has been suggested that a narrow upward fluid flow velocity of 20–60 cm yr^{-1} is required for MDAC formation in sulfatic sediments based on numerical modelling from Hydrate Ridge (Luff and Wallmann, 2003; Luff et al., 2004). Additional work focused on the methanogenic zone and globally distributed methane transport sites will benefit refinement of controlling factors for MDAC formation. There is also a critical need to constrain the TA/DIC dynamics of biogeochemical processes in methane-charged sediments, including their role in MDAC formation and dissolution. Refinement of TA vs DIC balance in methane-flux sites is necessary to verify and constrain the existing total MDAC accumulation rates. It has been well established that the SMTZ is not only a zone of AOM and MDAC formation but also a zone of interlinked biogeochemical processes involving OSR, sulfide burial, sulfide oxidation, carbonate dissolution, methanogenesis, trace metal cycling, etc. (Hong et al., 2013; Beulig et al., 2019; Smrzka et al., 2020). The overall effect of these processes on alkalinity consumption or production for carbonate precipitation and water column carbonate chemistry is not well constrained. For example, OSR under certain environmental conditions, aerobic methane oxidation, and aerobic sulfide oxidation can cause MDAC dissolution. In contrast, nitrate-driven sulfide oxidation, AOM, and deep alkalinity flux via MSiW can contribute to MDAC precipitation (Himmler et al., 2018; Loyd and Smirnoff, 2022). The relative balance of these processes in different flux settings needs to be determined to evaluate the role of MDAC formation and methane transport-induced biogeochemistry in ocean carbon chemistry.

Another largely unconstrained aspect of MDAC and methane-DIC cycling is the role of MSiW and the broader C-Si coupling in modern and past carbon cycling. The long-term evolution of C-Si coupling in the sediment column and its impact on carbon cycling is poorly constrained and methanogenic carbonates could offer an excellent archive to reconstruct such interactions. Recent studies have highlighted the strong tie of these processes in determining the upward cation and alkalinity flux on shallow sediment and bottom water biogeochemistry (Berg et al., 2019; Akam et al., 2020; Torres et al., 2020). Much of the studies so far emphasize how MSiW triggers formation of deep MDAC but essentially no study deals with how the acidity produced during

MDAC formation may further enhance MSiW and results in a positive feedback loop for MDAC accumulation. These initial results warrant a better quantitative understanding of C-Si coupling due to methanogenesis and MSiW, including their role in MDAC precipitation globally. Further, the extent of mixing of methanotrophic and methanogenic carbon sources determining $\delta^{13}C_{carb}$ of MDAC and is highly variable, potentially masking identification of MDAC in the sedimentary record. The need to expand the MDAC-search criteria from $\delta^{13}C$-centered to multi-proxy suites is also important as our current MDAC records are largely limited to geological conditions with sulfate and DIC concentration similar to modern levels producing ^{13}C-depletion (Bristow and Grotzinger, 2013). There is an evolving list of trace elements, biomarkers, petrographic, and additional isotope-based proxies to aid and expand our existing paleo-seep and MDAC records (Peckmann and Thiel, 2004; Lin et al., 2017; Smrzka et al., 2020; Hong et al., 2022; Peng et al., 2022). Lastly, the knowledge of MDAC in marine settings has also shown promise in wider directions including astrobiology and industrial application. Morphologic, geochemical, and microbial signatures of MDAC have been suggested as important templates for exobiology search on other planets and icy moons (Shapiro, 2004; Carrizo et al., 2022). Ganendra (Ganendra, 2015) suggested the potential of carbonate precipitation from methane oxidation as a more friendly approach towards bioconcrete solution to concrete cracks (Jain, 2021). Such prospects enhance the legacy of MDAC research to wider future directions.

Summary

We provided a synthesis on the biogeochemical importance of MDAC, authigenic carbonate minerals precipitating within anoxic marine environments with DIC and alkalinity derived primarily from methane oxidation and methane production. Incorporation of MDAC volume increases the marine carbonate burial budget in the continental margins by an average 10% (6–23%), an affect that was even larger in the geological past during events with widespread anoxia. MDAC provides an archive of the biogeochemical processes induced by methane-transport and particularly for C-S coupling, (i) in shallow sediments owing to SD-AOM and (ii) in deeper sediments due to C-Si coupling involving methanogenesis and marine silicate weathering. While MDAC sequesters a part of methane-derived DIC, it is a potential contributor to ocean acidification by the consumption of alkalinity from the benthic DIC flux in methane-laden sediments. MDAC was relevant to marine carbon biogeochemistry through most of geological history. Future studies need to quantify the volume of MDAC and the TA:DIC dynamics of related biogeochemical processes at present and over the geological past to elucidate the role of this carbonate factory in ocean's carbon biogeochemistry. Our concept on MDAC has evolved over the past five decades from a methane-derived carbon sequester in a seep-oasis setting to a dynamic carbonate factory with a spatial sphere of influence expanding from deep sediments to the water column and a temporal dimension from the Precambrian to present.

References

Akam, S.A., Coffin, R.B., Abdulla, H.A.N. and Lyons, T.W., 2020. Dissolved Inorganic Carbon Pump in Methane-Charged Shallow Marine Sediments: State of the Art and New Model Perspectives. Frontiers in Marine Science, 7(206).

Akam, S.A., Lyons, T.W., Coffin, R.B., McGee, D., Naehr, T.H., Bates, S.M., Clarkson, C. and Kiel Reese, B., 2021. Carbon-sulfur signals of methane versus crude oil diagenetic decomposition and U-Th age relationships for authigenic carbonates from asphalt seeps, southern Gulf of Mexico. Chemical Geology, 581: 120395.

Aloisi, G., Wallmann, K., Drews, M. and Bohrmann, G., 2004. Evidence for the submarine weathering of silicate minerals in Black Sea sediments: possible implications for the marine Li and B cycles. Geochemistry, Geophysics, Geosystems, 5(4).

Alt, J.C. and Teagle, D.A.H., 1999. The uptake of carbon during alteration of ocean crust. Geochimica et Cosmochimica Acta, 63(10): 1527-1535.

Andersson, A.J., 2014. 8.19 - The Oceanic CaCO3 Cycle. In: H.D. Holland and K.K. Turekian (Editors), Treatise on Geochemistry (Second Edition). Elsevier, Oxford, pp. 519-542.

Bayon, G., Pierre, C., Etoubleau, J., Voisset, M., Cauquil, E., Marsset, T., Sultan, N., Le Drezen, E. and Fouquet, Y., 2007. Sr/Ca and Mg/Ca ratios in Niger Delta sediments: Implications for authigenic carbonate genesis in cold seep environments. Marine Geology, 241(1-4): 93-109.

Bekker, A., Slack, J.F., Planavsky, N., Krapež, B., Hofmann, A., Konhauser, K.O. and Rouxel, O.J., 2010. Iron Formation: The Sedimentary Product of a Complex Interplay among Mantle, Tectonic, Oceanic, and Biospheric Processes*. Economic Geology, 105(3): 467-508.

Berg, R.D., Solomon, E.A. and Teng, F.-Z., 2019. The role of marine sediment diagenesis in the modern oceanic magnesium cycle. Nature communications, 10(1): 1-10.

Beulig, F., Roy, H., McGlynn, S.E. and Jorgensen, B.B., 2019. Cryptic CH4 cycling in the sulfate-methane transition of marine sediments apparently mediated by ANME-1 archaea. ISME J, 13(2): 250-262.

Birgel, D., Meister, P., Lundberg, R., Horath, T.D., Bontognali, T.R.R., Bahniuk, A.M., de Rezende, C.E., Vasconcelos, C. and McKenzie, J.A., 2015. Methanogenesis produces strong 13C enrichment in stromatolites of Lagoa Salgada, Brazil: a modern analogue for Palaeo-/Neoproterozoic stromatolites? Geobiology, 13(3): 245-266.

Boehme, S.E., Blair, N.E., Chanton, J.P. and Martens, C.S., 1996. A mass balance of 13C and 12C in an organic-rich methane-producing marine sediment. Geochimica et Cosmochimica Acta, 60(20): 3835-3848.

Boetius, A. and Wenzhöfer, F., 2013. Seafloor oxygen consumption fuelled by methane from cold seeps. Nature Geoscience, 6(9): 725-734.

Bohrmann, G. and Torres, M.E., 2014. Methane in Marine Sediments. In: J. Harff, M. Meschede, S. Petersen and J. Thiede (Editors), Encyclopedia of Marine Geosciences. Springer Netherlands, Dordrecht, pp. 1-7.

Borowski, W.S., Paull, C.K. and Ussler, W., 1996. Marine porewater sulfate profiles indicate in situ methane flux from underlying gas hydrate. Geology, 24(7): 655-658.

Bowles, M.W., Mogollón, J.M., Kasten, S., Zabel, M. and Hinrichs, K.-U., 2014. Global rates of marine sulfate reduction and implications for sub–seafloor metabolic activities. Science, 344(6186): 889-891.

Bradbury, H.J. and Turchyn, A.V., 2019. Reevaluating the carbon sink due to sedimentary carbonate formation in modern marine sediments. Earth and Planetary Science Letters, 519: 40-49.

Breitburg, D., Levin Lisa, A., Oschlies, A., Grégoire, M., Chavez Francisco, P., Conley Daniel, J., Garçon, V., Gilbert, D., Gutiérrez, D., Isensee, K., Jacinto Gil, S., Limburg Karin, E., Montes, I., Naqvi, S.W.A.,

539 Pitcher Grant, C., Rabalais Nancy, N., Roman Michael, R., Rose Kenneth, A., Seibel Brad, A.,
540 Telszewski, M., Yasuhara, M. and Zhang, J., 2018. Declining oxygen in the global ocean and
541 coastal waters. Science, 359(6371): eaam7240.
542 Brenner, H., Braeckman, U., Le Guitton, M. and Meysman, F.J., 2016. The impact of sedimentary
543 alkalinity release on the water column CO 2 system in the North Sea. Biogeosciences, 13(3): 841-
544 863.
545 Bristow, T.F. and Grotzinger, J.P., 2013. Sulfate availability and the geological record of cold-seep
546 deposits. Geology, 41(7): 811-814.
547 Cadeau, P., Jézéquel, D., Leboulanger, C., Fouilland, E., Le Floc'h, E., Chaduteau, C., Milesi, V., Guélard, J.,
548 Sarazin, G., Katz, A., d'Amore, S., Bernard, C. and Ader, M., 2020. Carbon isotope evidence for
549 large methane emissions to the Proterozoic atmosphere. Scientific Reports, 10(1): 18186.
550 Caesar, K.H., Kyle, J.R., Lyons, T.W., Tripati, A. and Loyd, S.J., 2019. Carbonate formation in salt dome cap
551 rocks by microbial anaerobic oxidation of methane. Nat Commun, 10(1): 808.
552 Cai, C., Li, K., Liu, D., John, C.M., Wang, D., Fu, B., Fakhraee, M., He, H., Feng, L. and Jiang, L., 2021.
553 Anaerobic oxidation of methane by Mn oxides in sulfate-poor environments. Geology, 49(7):
554 761-766.
555 Campbell, K.A., 2006. Hydrocarbon seep and hydrothermal vent paleoenvironments and paleontology:
556 past developments and future research directions. Palaeogeography, Palaeoclimatology,
557 Palaeoecology, 232(2): 362-407.
558 Carrizo, D., de Dios-Cubillas, A., Sánchez-García, L., López, I. and Prieto-Ballesteros, O., 2022.
559 Interpreting Molecular and Isotopic Biosignatures in Methane-Derived Authigenic Carbonates in
560 the Light of a Potential Carbon Cycle in the Icy Moons. Astrobiology, 22(5): 552-567.
561 Cavicchioli, R., Ripple, W.J., Timmis, K.N., Azam, F., Bakken, L.R., Baylis, M., Behrenfeld, M.J., Boetius, A.,
562 Boyd, P.W., Classen, A.T., Crowther, T.W., Danovaro, R., Foreman, C.M., Huisman, J., Hutchins,
563 D.A., Jansson, J.K., Karl, D.M., Koskella, B., Mark Welch, D.B., Martiny, J.B.H., Moran, M.A.,
564 Orphan, V.J., Reay, D.S., Remais, J.V., Rich, V.I., Singh, B.K., Stein, L.Y., Stewart, F.J., Sullivan,
565 M.B., van Oppen, M.J.H., Weaver, S.C., Webb, E.A. and Webster, N.S., 2019. Scientists' warning
566 to humanity: microorganisms and climate change. Nature Reviews Microbiology, 17(9): 569-586.
567 Chen, F., Wang, X., Li, N., Cao, J., Bayon, G., Peckmann, J., Hu, Y., Gong, S., Cheng, H. and Edwards, R.L.,
568 2019. Gas hydrate dissociation during sea-level highstand inferred from U/Th dating of seep
569 carbonate from the South China Sea. Geophysical Research Letters, 46(23): 13928-13938.
570 Ciais, P., Chris, S., Govindasamy, B., Bopp, L., Brovkin, V., Canadell, J., Chhabra, A., Defries, R., Galloway,
571 J. and Heimann, M., 2013. Carbon and other biogeochemical cycles. Climate Change 2013: The
572 Physical Science Basis: 465-570.
573 Claypool, G.E. and Kaplan, I., 1974. The origin and distribution of methane in marine sediments, Natural
574 gases in marine sediments. Springer, pp. 99-139.
575 Cordova-Gonzalez, A., Birgel, D., Wisshak, M., Urich, T., Brinkmann, F., Marcon, Y., Bohrmann, G. and
576 Peckmann, J., 2023. A carbonate corrosion experiment at a marine methane seep: The role of
577 aerobic methanotrophic bacteria. Geobiology, n/a(n/a).
578 Cui, H., Kaufman, A.J., Xiao, S., Zhou, C. and Liu, X.-M., 2017. Was the Ediacaran Shuram Excursion a
579 globally synchronized early diagenetic event? Insights from methane-derived authigenic
580 carbonates in the uppermost Doushantuo Formation, South China. Chemical Geology, 450: 59-
581 80.
582 Cui, H., Kitajima, K., Orland, I.J., Baele, J.-M., Xiao, S., Kaufman, A.J., Denny, A., Spicuzza, M.J., Fournelle,
583 J.H. and Valley, J.W., 2022. An authigenic response to Ediacaran surface oxidation: Remarkable
584 micron-scale isotopic heterogeneity revealed by SIMS. Precambrian Research, 377: 106676.

585 Dickens, G.R., 2011. Down the rabbit hole: Toward appropriate discussion of methane release from gas
586 hydrate systems during the Paleocene-Eocene thermal maximum and other past hyperthermal
587 events. Climate of the Past, 7(3): 831-846.
588 Egger, M., Riedinger, N., Mogollón, J.M. and Jørgensen, B.B., 2018. Global diffusive fluxes of methane in
589 marine sediments. Nature Geoscience, 11(6): 421.
590 Falkowski, P., Scholes, R., Boyle, E., Canadell, J., Canfield, D., Elser, J., Gruber, N., Hibbard, K., Högberg, P.
591 and Linder, S., 2000. The global carbon cycle: a test of our knowledge of earth as a system.
592 science, 290(5490): 291-296.
593 Frank, T.D. and Lyons, T.W., 1998. "Molar-tooth" structures: A geochemical perspective on a Proterozoic
594 enigma. Geology, 26(8): 683-686.
595 Ganendra, G., 2015. Housing methane-oxidizing bacteria on building materials: towards a sustainable air
596 bioremediation and building materials surface protection.
597 Haig, D.W., Dillinger, A., Playford, G., Riera, R., Sadekov, A., Skrzypek, G., Håkansson, E., Mory, A.J.,
598 Peyrot, D. and Thomas, C., 2022. Methane seeps following Early Permian (Sakmarian)
599 deglaciation, interior East Gondwana, Western Australia: Multiphase carbonate cements,
600 distinct carbon-isotope signatures, extraordinary biota. Palaeogeography, Palaeoclimatology,
601 Palaeoecology, 591: 110862.
602 Haqq-Misra, J.D., Domagal-Goldman, S.D., Kasting, P.J. and Kasting, J.F., 2008. A Revised, Hazy Methane
603 Greenhouse for the Archean Earth. Astrobiology, 8(6): 1127-1137.
604 Hathaway, J.C. and Degens, E.T., 1969. Methane-Derived Marine Carbonates of Pleistocene Age.
605 Science, 165(3894): 690-692.
606 Hayes, J.M. and Waldbauer, J.R., 2006. The carbon cycle and associated redox processes through time.
607 Philosophical Transactions of the Royal Society B: Biological Sciences, 361(1470): 931-950.
608 Hein, J.R. and Koski, R.A., 1987. Bacterially mediated diagenetic origin for chert-hosted manganese
609 deposits in the Franciscan Complex, California Coast Ranges. Geology, 15(8): 722-726.
610 Higgins, J.A., Fischer, W. and Schrag, D., 2009. Oxygenation of the ocean and sediments: consequences
611 for the seafloor carbonate factory. Earth and Planetary Science Letters, 284(1-2): 25-33.
612 Himmler, T., Bach, W., Bohrmann, G. and Peckmann, J., 2010. Rare earth elements in authigenic
613 methane-seep carbonates as tracers for fluid composition during early diagenesis. Chemical
614 Geology, 277(1-2): 126-136.
615 Himmler, T., Bayon, G., Wangner, D., Enzmann, F., Peckmann, J. and Bohrmann, G., 2016. Seep-
616 carbonate lamination controlled by cyclic particle flux. Scientific Reports, 6.
617 Himmler, T., Smrzka, D., Zwicker, J., Kasten, S., Shapiro, R.S., Bohrmann, G. and Peckmann, J., 2018.
618 Stromatolites below the photic zone in the northern Arabian Sea formed by calcifying
619 chemotrophic microbial mats. Geology, 46(4): 339-342.
620 Hong, W.-L., Lepland, A., Kirsimäe, K., Crémière, A. and Rae, J.W.B., 2022. Boron concentrations and
621 isotopic compositions in methane-derived authigenic carbonates: Constraints and limitations in
622 reconstructing formation conditions. Earth and Planetary Science Letters, 579: 117337.
623 Hong, W.-L., Torres, M.E., Kim, J.-H., Choi, J. and Bahk, J.-J., 2013. Carbon cycling within the sulfate-
624 methane-transition-zone in marine sediments from the Ulleung Basin. Biogeochemistry, 115(1-
625 3): 129-148.
626 Hong, W.-L., Torres, M.E., Kim, J.-H., Choi, J. and Bahk, J.-J., 2014. Towards quantifying the reaction
627 network around the sulfate–methane-transition-zone in the Ulleung Basin, East Sea, with a
628 kinetic modeling approach. Geochimica et Cosmochimica Acta, 140: 127-141.
629 Hu, X. and Cai, W.J., 2011. An assessment of ocean margin anaerobic processes on oceanic alkalinity
630 budget. Global Biogeochemical Cycles, 25(3).

631 Hu, Y., Feng, D., Peckmann, J., Zhang, X., Chen, L., Feng, J., Wang, H. and Chen, D., 2023. The crucial role
632 of deep-sourced methane in maintaining the subseafloor sulfate budget. Geoscience Frontiers,
633 14(3): 101530.
634 Hu, Y., Zhang, X., Feng, D., Peckmann, J., Feng, J., Wang, H., Yang, S. and Chen, D., 2022. Enhanced
635 sulfate consumption fueled by deep-sourced methane in a hydrate-bearing area. Science
636 Bulletin, 67(2): 122-124.
637 Isson, T.T. and Planavsky, N.J., 2018. Reverse weathering as a long-term stabilizer of marine pH and
638 planetary climate. Nature, 560(7719): 471-475.
639 Jain, S., 2021. An Overview of Factors Influencing Microbially Induced Carbonate Precipitation for Its
640 Field Implementation. In: V. Achal and C.S. Chin (Editors), Building Materials for Sustainable and
641 Ecological Environment. Springer Singapore, Singapore, pp. 73-99.
642 Jakubowicz, M., Hryniewicz, K. and Belka, Z., 2017. Mass occurrence of seep-specific bivalves in the
643 oldest-known cold seep metazoan community. Scientific Reports, 7(1): 14292.
644 Jiang, G., Kennedy, M.J. and Christie-Blick, N., 2003. Stable isotopic evidence for methane seeps in
645 Neoproterozoic postglacial cap carbonates. Nature, 426(6968): 822-826.
646 Jilbert, T., Cowie, G., Lintumäki, L., Jokinen, S., Asmala, E., Sun, X., Mörth, C.-M., Norkko, A. and
647 Humborg, C., 2021. Anthropogenic Inputs of Terrestrial Organic Matter Influence Carbon
648 Loading and Methanogenesis in Coastal Baltic Sea Sediments. Frontiers in Earth Science, 9.
649 Jørgensen, B.B. and Kasten, S., 2006. Sulfur Cycling and Methane Oxidation. In: H.D. Schulz and M. Zabel
650 (Editors), Marine Geochemistry. Springer Berlin Heidelberg, Berlin, Heidelberg, pp. 271-309.
651 Judd, A. and Hovland, M., 2007. Seabed Fluid Flow: The Impact on Geology, Biology and the Marine
652 Environment. Cambridge University Press, Cambridge.
653 Kennedy, M., Mrofka, D. and von der Borch, C., 2008. Snowball Earth termination by destabilization of
654 equatorial permafrost methane clathrate. Nature, 453(7195): 642-645.
655 Kharecha, P., Kasting, J. and Siefert, J., 2005. A coupled atmosphere–ecosystem model of the early
656 Archean Earth. Geobiology, 3(2): 53-76.
657 Kriscautzky, A., Kah, L.C. and Bartley, J.K., 2022. Molar-Tooth Structure as a Window into the Deposition
658 and Diagenesis of Precambrian Carbonate. Annual Review of Earth and Planetary Sciences,
659 50(1): 205-230.
660 Krumins, V., Gehlen, M., Arndt, S., Cappellen, P.V. and Regnier, P., 2013. Dissolved inorganic carbon and
661 alkalinity fluxes from coastal marine sediments: model estimates for different shelf
662 environments and sensitivity to global change. Biogeosciences, 10(1): 371-398.
663 Laakso, T.A. and Schrag, D.P., 2020. The role of authigenic carbonate in Neoproterozoic carbon isotope
664 excursions. Earth and Planetary Science Letters, 549: 116534.
665 Labrado, A.L., Brunner, B., Bernasconi, S.M. and Peckmann, J., 2019. Formation of large native sulfur
666 deposits does not require molecular oxygen. Frontiers in Microbiology, 10.
667 Lepot, K., Williford, K.H., Philippot, P., Thomazo, C., Ushikubo, T., Kitajima, K., Mostefaoui, S. and Valley,
668 J.W., 2019. Extreme 13C-depletions and organic sulfur content argue for S-fueled anaerobic
669 methane oxidation in 2.72 Ga old stromatolites. Geochimica et Cosmochimica Acta, 244: 522-
670 547.
671 Leprich, D.J., Flood, B.E., Schroedl, P.R., Ricci, E., Marlow, J.J., Girguis, P.R. and Bailey, J.V., 2021. Sulfur
672 bacteria promote dissolution of authigenic carbonates at marine methane seeps. The ISME
673 Journal.
674 Levin, L.A., Baco, A.R., Bowden, D.A., Colaco, A., Cordes, E.E., Cunha, M.R., Demopoulos, A.W., Gobin, J.,
675 Grupe, B.M. and Le, J., 2016. Hydrothermal vents and methane seeps: rethinking the sphere of
676 influence. Frontiers in Marine Science, 3: 72.
677 Lin, Z., Sun, X., Strauss, H., Lu, Y., Gong, J., Xu, L., Lu, H., Teichert, B.M.A. and Peckmann, J., 2017.
678 Multiple sulfur isotope constraints on sulfate-driven anaerobic oxidation of methane: Evidence

679 from authigenic pyrite in seepage areas of the South China Sea. Geochimica et Cosmochimica
680 Acta, 211: 153-173.
681 Loyd, S.J. and Smirnoff, M.N., 2022. Progressive formation of authigenic carbonate with depth in
682 siliciclastic marine sediments including substantial formation in sediments experiencing
683 methanogenesis. Chemical Geology, 594: 120775-120775.
684 Luff, R. and Wallmann, K., 2003. Fluid flow, methane fluxes, carbonate precipitation and biogeochemical
685 turnover in gas hydrate-bearing sediments at Hydrate Ridge, Cascadia Margin: numerical
686 modeling and mass balances. Geochimica et Cosmochimica Acta, 67(18): 3403-3421.
687 Luff, R., Wallmann, K. and Aloisi, G., 2004. Numerical modeling of carbonate crust formation at cold vent
688 sites: significance for fluid and methane budgets and chemosynthetic biological communities.
689 Earth and Planetary Science Letters, 221(1-4): 337-353.
690 Marlow, J., Hoer, D., Jungbluth Sean, P., Reynard Linda, M., Gartman, A., Chavez Marko, S., El-Naggar
691 Mohamed, Y., Tuross, N., Orphan Victoria, J. and Girguis Peter, R., 2021. Carbonate-hosted
692 microbial communities are prolific and pervasive methane oxidizers at geologically diverse
693 marine methane seep sites. Proceedings of the National Academy of Sciences, 118(25):
694 e2006857118.
695 Marlow, J.J., Anderson, R.E., Reysenbach, A.-L., Seewald, J.S., Shank, T.M., Teske, A.P., Wanless, V.D. and
696 Soule, S.A., 2022. New Opportunities and Untapped Scientific Potential in the Abyssal Ocean.
697 Frontiers in Marine Science, 8.
698 Maslin, M., Mikkelsen, N., Vilela, C. and Haq, B., 1998. Sea-level –and gas-hydrate–controlled
699 catastrophic sediment failures of the Amazon Fan. Geology, 26(12): 1107-1110.
700 Matsumoto, R., 1990. Vuggy carbonate crust formed by hydrocarbon seepage on the continental shelf of
701 Baffin Island, northeast Canada. Geochemical Journal, 24(3): 143-158.
702 Meister, P., 2013. Two opposing effects of sulfate reduction on carbonate precipitation in normal
703 marine, hypersaline, and alkaline environments. Geology, 41(4): 499-502.
704 Meister, P., Herda, G., Petrishcheva, E., Gier, S., Dickens, G.R., Bauer, C. and Liu, B., 2022. Microbial
705 Alkalinity Production and Silicate Alteration in Methane Charged Marine Sediments: Implications
706 for Porewater Chemistry and Diagenetic Carbonate Formation. Frontiers in Earth Science, 9.
707 Meister, P., Liu, B., Ferdelman, T.G., Jørgensen, B.B. and Khalili, A., 2013. Control of sulphate and
708 methane distributions in marine sediments by organic matter reactivity. Geochimica et
709 Cosmochimica Acta, 104: 183-193.
710 Meister, P., Liu, B., Khalili, A., Böttcher, M.E. and Jørgensen, B.B., 2019. Factors controlling the carbon
711 isotope composition of dissolved inorganic carbon and methane in marine porewater: An
712 evaluation by reaction-transport modelling. Journal of Marine Systems, 200: 103227.
713 Meister, P. and Reyes, C., 2019. The Carbon-Isotope Record of the Sub-Seafloor Biosphere. Geosciences,
714 9(12).
715 Michaelis, W., Seifert, R., Nauhaus, K., Treude, T., Thiel, V., Blumenberg, M., Knittel, K., Gieseke, A.,
716 Peterknecht, K., Pape, T., Boetius, A., Amann, R., Jørgensen Bo, B., Widdel, F., Peckmann, J.,
717 Pimenov Nikolai, V. and Gulin Maksim, B., 2002. Microbial Reefs in the Black Sea Fueled by
718 Anaerobic Oxidation of Methane. Science, 297(5583): 1013-1015.
719 Michel, J., Laugié, M., Pohl, A., Lanteaume, C., Masse, J.-P., Donnadieu, Y. and Borgomano, J., 2019.
720 Marine carbonate factories: a global model of carbonate platform distribution. International
721 Journal of Earth Sciences, 108(6): 1773-1792.
722 Middelburg, J.J., Soetaert, K. and Hagens, M., 2020. Ocean Alkalinity, Buffering and Biogeochemical
723 Processes. Reviews of Geophysics, 58(3): e2019RG000681.
724 Müller, G., Börker, J., Sluijs, A. and Middelburg, J.J., 2022. Detrital Carbonate Minerals in Earth's Element
725 Cycles. Global Biogeochemical Cycles, 36(5): e2021GB007231.

Naehr, T.H., Eichhubl, P., Orphan, V.J., Hovland, M., Paull, C.K., Ussler Iii, W., Lorenson, T.D. and Greene, H.G., 2007. Authigenic carbonate formation at hydrocarbon seeps in continental margin sediments: A comparative study. Deep Sea Research Part II: Topical Studies in Oceanography, 54(11-13): 1268-1291.

Oppo, D., De Siena, L. and Kemp, D.B., 2020. A record of seafloor methane seepage across the last 150 million years. Scientific Reports, 10(1): 2562.

Osborne, E., Hu, X., Hall, E.R., Yates, K., Vreeland-Dawson, J., Shamberger, K., Barbero, L., Martin Hernandez-Ayon, J., Gomez, F.A., Hicks, T., Xu, Y.-Y., McCutcheon, M.R., Acquafredda, M., Chapa-Balcorta, C., Norzagaray, O., Pierrot, D., Munoz-Caravaca, A., Dobson, K.L., Williams, N., Rabalais, N. and Dash, P., 2022. Ocean acidification in the Gulf of Mexico: Drivers, impacts, and unknowns. Progress in Oceanography, 209: 102882.

Peckmann, J., Campbell, K.A., Walliser, O.H. and Reitner, J., 2007. A Late Devonian Hydrocarbon-Seep Deposit Dominated by Dimerelloid Brachiopods, Morocco. PALAIOS, 22(2): 114-122.

Peckmann, J., Kiel, S., Sandy, M.R., Taylor, D.G. and Goedert, J.L., 2011. Mass Occurrences of the Brachiopod Halorella in Late Triassic Methane-Seep Deposits, Eastern Oregon. The Journal of Geology, 119(2): 207-220.

Peckmann, J. and Thiel, V., 2004. Carbon cycling at ancient methane–seeps. Chemical Geology, 205(3): 443-467.

Peng, X., Guo, Z., Chen, S., Sun, Z., Xu, H., Ta, K., Zhang, J., Zhang, L., Li, J. and Du, M., 2017. Formation of carbonate pipes in the northern Okinawa Trough linked to strong sulfate exhaustion and iron supply. Geochimica et Cosmochimica Acta, 205: 1-13.

Peng, Y., Bao, H., Jiang, G., Crockford, P., Feng, D., Xiao, S., Kaufman Alan, J. and Wang, J., 2022. A transient peak in marine sulfate after the 635-Ma snowball Earth. Proceedings of the National Academy of Sciences, 119(19): e2117341119.

Portnov, A., Vadakkepuliyambatta, S., Mienert, J. and Hubbard, A., 2016. Ice-sheet-driven methane storage and release in the Arctic. Nature Communications, 7(1): 10314.

Prouty, N., Brothers, D., Kluesner, J., Barrie, J., Andrews, B., Lauer, R., Greene, H., Conrad, J., Lorenson, T., Law, M., Sahy, D., Conway, K., McGann, M. and Dartnell, P., 2020. Focused fluid flow and methane venting along the Queen Charlotte fault, offshore Alaska (USA) and British Columbia (Canada). Geosphere.

Reeburgh, W.S., 1976. Methane consumption in Cariaco Trench waters and sediments. Earth and Planetary Science Letters, 28(3): 337-344.

Renard, M., Rafélis, M., Emmanuel, L., Moullade, M., Masse, J.-P., Kuhnt, W., Bergen, J. and Tronchetti, G., 2005. Early Aptian δ13C and manganese anomalies from the historical Cassis-La Bédoule stratotype sections (S.E. France): relationship with a methane hydrate dissociation event and stratigraphic implications. Carnets de géologie (Notebooks on geology), 24.

Roberts, H.H. and Carney, R.S., 1997. Evidence of episodic fluid, gas, and sediment venting on the northern Gulf of Mexico continental slope. Economic Geology, 92(7-8): 863-879.

Roberts, H.H. and Feng, D., 2013. Carbonate Precipitation at Gulf of Mexico Hydrocarbon Seeps: An Overview, Hydrocarbon Seepage: From Source to Surface. SEG and AAPG, pp. 43-61.

Ruppel, C.D. and Kessler, J.D., 2017. The interaction of climate change and methane hydrates. Reviews of Geophysics, 55(1): 126-168.

Saitoh, M., Ueno, Y., Isozaki, Y., Shibuya, T., Yao, J., Ji, Z., Shozugawa, K., Matsuo, M. and Yoshida, N., 2015. Authigenic carbonate precipitation at the end-Guadalupian (Middle Permian) in China: Implications for the carbon cycle in ancient anoxic oceans. Progress in Earth and Planetary Science, 2(1): 41.

Santos, I.R., Burdige, D.J., Jennerjahn, T.C., Bouillon, S., Cabral, A., Serrano, O., Wernberg, T., Filbee-Dexter, K., Guimond, J.A. and Tamborski, J.J., 2021. The renaissance of Odum's outwelling hypothesis in 'Blue Carbon' science. Estuarine, Coastal and Shelf Science, 255: 107361.

Schrag, D.P., Higgins, J.A., Macdonald, F.A. and Johnston, D.T., 2013. Authigenic carbonate and the history of the global carbon cycle. Science, 339(6119): 540-3.

Shapiro, R., 2004. Recognition of Fossil Prokaryotes in Cretaceous Methane Seep Carbonates: Relevance to Astrobiology. Astrobiology, 4(4): 438-449.

Shen, B., Dong, L., Xiao, S., Lang, X., Huang, K., Peng, Y., Zhou, C., Ke, S. and Liu, P., 2016. Molar tooth carbonates and benthic methane fluxes in Proterozoic oceans. Nature Communications, 7(1): 10317.

Smrzka, D., Feng, D., Himmler, T., Zwicker, J., Hu, Y., Monien, P., Tribovillard, N., Chen, D. and Peckmann, J., 2020. Trace elements in methane-seep carbonates: Potentials, limitations, and perspectives. Earth-Science Reviews, 208: 103263.

Smrzka, D., Zwicker, J., Lu, Y., Sun, Y., Feng, D., Monien, P., Bohrmann, G. and Peckmann, J., 2021. Trace element distribution in methane-seep carbonates: The role of mineralogy and dissolved sulfide. Chemical Geology: 120357.

Smrzka, D., Zwicker, J., Misch, D., Walkner, C., Gier, S., Monien, P., Bohrmann, G. and Peckmann, J., 2019. Oil seepage and carbonate formation: A case study from the southern Gulf of Mexico. Sedimentology.

Solomon, E.A., Spivack, A.J., Kastner, M., Torres, M.E. and Robertson, G., 2014. Gas hydrate distribution and carbon sequestration through coupled microbial methanogenesis and silicate weathering in the Krishna–Godavari basin, offshore India. Marine and Petroleum Geology, 58: 233-253.

Suess, E., 2014. Marine cold seeps and their manifestations: geological control, biogeochemical criteria and environmental conditions. International Journal of Earth Sciences, 103(7): 1889-1916.

Sun, X. and Turchyn, A.V., 2014. Significant contribution of authigenic carbonate to marine carbon burial. Nature Geoscience, 7(3): 201-204.

Sun, Z., Wei, H., Zhang, X., Shang, L., Yin, X., Sun, Y., Xu, L., Huang, W. and Zhang, X., 2015. A unique Fe-rich carbonate chimney associated with cold seeps in the Northern Okinawa Trough, East China Sea. Deep Sea Research Part I: Oceanographic Research Papers, 95: 37-53.

Swanner, E.D., Lambrecht, N., Wittkop, C., Harding, C., Katsev, S., Torgeson, J. and Poulton, S.W., 2020. The biogeochemistry of ferruginous lakes and past ferruginous oceans. Earth-Science Reviews, 211: 103430.

Talukder, A.R., 2012. Review of submarine cold seep plumbing systems: leakage to seepage and venting. Terra Nova, 24(4): 255-272.

Tang, D., Fang, H., Shi, X., Liang, L., Zhou, L., Xie, B., Huang, K., Zhou, X., Wu, M. and Riding, R., 2023. Mesoproterozoic Molar Tooth Structure Related to Increased Marine Oxygenation. Journal of Geophysical Research: Biogeosciences, 128(1): e2022JG007077.

Thomas, H., Schiettecatte, L., Suykens, K., M Kone, Y., Shadwick, E., F Prowe, A., Bozec, Y., W de Baar, H. and Borges, A., 2008. Enhanced ocean carbon storage from anaerobic alkalinity generation in coastal sediments. Biogeosciences Discussions.

Torres, M.E., Hong, W.-L., Solomon, E.A., Milliken, K., Kim, J.-H., Sample, J.C., Teichert, B.M.A. and Wallmann, K., 2020. Silicate weathering in anoxic marine sediment as a requirement for authigenic carbonate burial. Earth-Science Reviews, 200: 102960.

Turchyn, A.V., Bradbury, H.J., Walker, K. and Sun, X., 2021. Controls on the Precipitation of Carbonate Minerals Within Marine Sediments. Frontiers in Earth Science, 9.

Wallmann, K., Aloisi, G., Haeckel, M., Tishchenko, P., Pavlova, G., Greinert, J., Kutterolf, S. and Eisenhauer, A., 2008. Silicate weathering in anoxic marine sediments. Geochimica et Cosmochimica Acta, 72(12): 2895-2918.

Wallmann, K., Riedel, M., Hong, W.L., Patton, H., Hubbard, A., Pape, T., Hsu, C.W., Schmidt, C., Johnson, J.E., Torres, M.E., Andreassen, K., Berndt, C. and Bohrmann, G., 2018. Gas hydrate dissociation off Svalbard induced by isostatic rebound rather than global warming. Nature Communications, 9(1): 83.

Wittkop, C., Swanner, E.D., Grengs, A., Lambrecht, N., Fakhraee, M., Myrbo, A., Bray, A.W., Poulton, S.W. and Katsev, S., 2020. Evaluating a primary carbonate pathway for manganese enrichments in reducing environments. Earth and Planetary Science Letters, 538: 116201.

Xu, S., Sun, Z., Geng, W., Cao, H., Zhang, X., Zhai, B. and Wu, Z., 2022. Advance in Numerical Simulation Research of Marine Methane Processes. Frontiers in Earth Science, 10.

Yao, H., Chen, X., Brunner, B., Birgel, D., Lu, Y., Guo, H., Wang, C. and Peckmann, J., 2022. Hydrocarbon seepage in the mid-Cretaceous greenhouse world: A new perspective from southern Tibet. Global and Planetary Change, 208: 103683.

Zhang, S., 2020. The relationship between organoclastic sulfate reduction and carbonate precipitation/dissolution in marine sediments. Marine Geology, 428: 106284.

Zhang, Y., Luo, M., Hu, Y., Wang, H. and Chen, D., 2019. An Areal Assessment of Subseafloor Carbon Cycling in Cold Seeps and Hydrate-Bearing Areas in the Northern South China Sea. Geofluids, 2019.

Zhou, X., Li, R., Tang, D., Huang, K.-J., Liu, K. and Ding, Y., 2022. Cold seep activity in the early Cambrian: evidence from the world-class shale-hosted Tianzhu barite deposit, South China. Sedimentary Geology: 106220.